

# Conceptual design of the satellite payload for the JASMINE mission

Hirokazu Kataza<sup>a</sup>, Ryouhei Kano<sup>b</sup>, Naoteru Gouda<sup>b</sup>, Masayuki Hirabayashi<sup>b</sup>, Naoki Isobe<sup>a</sup>, Takafumi Kamizuka<sup>c</sup>, Shingo Kashima<sup>b</sup>, Hajime Kawahara<sup>a</sup>, Daisuke Kawata<sup>d</sup>, Naoki Kohara<sup>b</sup>, Iona Kondo<sup>a</sup>, Ichiro Mase<sup>b</sup>, Kohei Miyakawa<sup>b</sup>, Ryou Ohsawa<sup>b</sup>, Masanobu Ozaki<sup>b</sup>, Risa Shimizu<sup>b</sup>, Yoshinori Suematsu<sup>b</sup>, Shotaro Tada<sup>e</sup>, Toshihiro Tsuzuki<sup>b</sup>, Fumihiro Uraguchi<sup>b</sup>, Fumihiko Usui<sup>a</sup>, Shin Utsunomiya<sup>b</sup>, Takehiko Wada<sup>b</sup>, Yoshiyuki Yamada<sup>f</sup>, and Taihei Yano<sup>b</sup>

<sup>a</sup>Institute of Space and Astronautical Science, Japan Aerospace Exploration Agency, 3-1-1, Yoshinodai, Chuo-ku, Sagami-hara, Kanagawa 252-5210, Japan

<sup>b</sup>National Astronomical Observatory of Japan, 2-21-1 Osawa, Mitaka, Tokyo 181-8588, Japan

<sup>c</sup>Institute of Astronomy, The Univ. of Tokyo, 2-21-1 Osawa, Mitaka, Tokyo 181-0015, Japan

<sup>d</sup>Mullard Space Science Lab., Univ. College London, Holmbury St. Mary Dorking, Surrey RH5 6NT, United Kingdom

<sup>e</sup>The Graduate Univ. for Advanced Studies, Shonan Village, Hayama, Kanagawa 240-0193, Japan

<sup>f</sup>Kyoto Univ. Yoshida-honmachi, Sakyo-ku, Kyoto 606-8501, Japan

## ABSTRACT

To investigate the evolution of our Galaxy, we plan to measure the distances and motions of stars in the Galactic center region. Additionally, our goal is to detect planets within the habitable zone around mid-M-type stars using transit phenomena. To achieve these objectives, we initiated the Japan Astrometry Satellite Mission for Infrared Exploration (JASMINE) project, targeting a 40 microarcsecond annual parallax measurement and aiming photometric accuracy of less than 0.3% for mid-M-type stars. A conceptual study of the observation instrument was conducted. As a result, the telescope is designed with high stability in orbit through carefully chosen materials and a special thermal design. A three-year operation is planned to collect sufficient data for annual parallax measurements. The telescope, with a diameter of 36 cm, covers wavelengths from 1.0 to 1.6 microns using InGaAs detectors. This paper will detail how instrument parameters were selected based on scientific objectives.

## 1. INTRODUCTION

The JASMINE mission has two main scientific objectives. First, to study the formation and evolution of the Milky Way, the mission aims to obtain high-precision distance and motion information of stars in the central core region. To achieve this, the mission will create an astrometric data catalog that includes annual parallax and proper motion, derived from the time series data of stellar positional variations on the celestial sphere.

Second, as an initial step towards observing the atmospheres of exoplanets located in habitable zones, the mission aims to detect transit phenomena of exoplanets in these zones. To this end, photometric observations of mid-type M stars will be conducted, and the time series photometric data will be made publicly available.

The Galactic center region has been extensively observed using ground-based telescopes, and information such as the positions, brightness, and colors of stars within this region has already been cataloged. Therefore, the list of celestial objects in the Galactic center region to be observed by JASMINE already exists, and JASMINE will refine the positional information of these pre-existing stellar lists.

---

Further author information: (Send correspondence to H.K.)

H.K.: E-mail: kataza@ir.isas.jaxa.jp, Telephone: 81 70 1170 2742

Space Telescopes and Instrumentation 2024: Optical, Infrared, and Millimeter Wave,  
edited by Laura E. Coyle, Shuji Matsuura, Marshall D. Perrin, Proc. of SPIE Vol.  
13092, 130920A · © 2024 SPIE · 0277-786X · doi: 10.1117/12.3018609

Moreover, the Gaia mission<sup>1</sup> has measured positional, kinematic, and photometric data of stars in visible wavelengths. Although Gaia data is unavailable for stars at the Galactic center due to interstellar absorption, the positional data of stars in the foreground, along the line of sight to the Galactic center, has been observed with approximately 20  $\mu\text{as}$  accuracy. These Gaia data will be used to calibrate the coordinate system of JASMINE.

The target for transit observations is Earth-like planets located in habitable zones, where liquid water can be maintained on their surfaces. These planets orbit stars smaller than the Sun (mid-type M stars). If transit planets are detected, follow-up observations using large telescopes can enable the search for life.

In addition to these two primary objectives, the mission encompasses a wide range of potential scientific research areas and highlights synergies with other missions, as detailed in the White Paper.<sup>2</sup>

## 2. TARGETS AND CONSTRAINTS

The target of the JASMINE mission is to publish an astrometric data catalog and time-series photometric data.

The astrometric observations will focus on the Galactic center region, defined by the coordinates  $-1.4^\circ < l < 0.7^\circ$  and  $-0.6^\circ < b < 0.6^\circ$  in galactic longitude ( $l$ ) and latitude ( $b$ ), respectively. In this region, the mission aims to measure the annual parallax with an accuracy of 40  $\mu\text{as}$  for over 2,400 stars in the Galactic center and the proper motion with an accuracy of 125  $\mu\text{as}/\text{yr}$  for over 45,000 stars in the Galactic center. Additionally, as an extra success level, the mission sets the goal of achieving an annual parallax measurement accuracy of 25  $\mu\text{as}$ .

For the transit observations, the mission requires time-series photometric observations capable of detecting a brightness decrease of less than 0.3% over a total observation period of 14 months for more than 17 mid-M-type stars that meet the criteria for candidate observation targets.

The mission is subject to the following constraints. The launch capability of the available rocket is assumed to be capable of deploying a 600 kg satellite into a Sun-synchronous orbit (SSO) at an altitude of 600 km. The project is under stringent budgetary constraints, necessitating the realization of the mission at the minimum cost within the requirements of the mission.

## 3. BASIC CONCEPT

Due to significant interstellar absorption toward the Galactic center, the number of observable stars in this region is very limited in visible light. To observe the required number of stars, near-infrared observations are suitable, as stellar photospheric emission is sufficient and interstellar absorption is minimal. Near-infrared observations are also expected to provide high sensitivity to mid-type M stars, which are difficult to target adequately with other wavelengths for exoplanet transit observations. Conducting observations of previously undetected transit phenomena through precise photometry is advantageous with space telescopes compared to ground-based telescopes.

To measure the relative positions of stars with high precision, there are three approaches: (1) imaging observations using a single-field telescope, (2) imaging observations using a two-field telescope with a large angular separation, and (3) relative position measurements with high angular resolution using an interferometer. We have focused on the single-field telescope imaging observations for the following reasons. The two-field telescope method with a large angular separation was employed by previous astrometric satellites, Hipparcos and Gaia. This method is excellent for accurately measuring stellar positions based on all-sky observations. However, for JASMINE, which has an observation region limited to within a few degrees, the scientific value of the observation data from one of the two fields is minimal. Furthermore, the interferometer method (3) has a field of view limited to a few arcseconds, and current technology makes its implementation in infrared wavelengths in space extremely challenging. Considering these factors, the single-field telescope imaging observations (1) are the most suitable for JASMINE as a small-scale mission focused on the Galactic center region.

Next, we adopted the step-stare method, which involves taking images in a specific direction and then shifting the pointing direction to cover the entire observation region with multiple images. This method was chosen for the following reasons.

The required field of view for the Galactic center region is approximately 1 square degree. Achieving sub-arcsecond resolution across this entire region within a telescope's single shot field of view is very difficult. For areas that cannot be covered by a single shot field of view, there are two methods: (1) the step-stare method, and (2) the Time Delay Integration (TDI) method, which moves the pointing direction slightly while integrating the signal. While TDI is feasible with visible light CCD detectors, it is not currently achievable with infrared CMOS detectors. Therefore, JASMINE will use the step-stare method. This method also allows for efficient transit observations by fixing the pointing direction for multiple observations, making it suitable for both types of observations.

As a result of adopting the step-stare method using a single field-of-view telescope, the following two requirements are necessitated:

Firstly, it is essential to obtain a good Point Spread Function (PSF). In JASMINE, both optical effects and pointing disturbances affect the PSF. In astrometric observations, the relative positions of stars obtained through imaging are used. The PSF is estimated using multiple images within a single exposure in the step-stare method. Therefore, it is crucial to obtain sharp and uniform star images across the entire field of view. Additionally, the sensitivity of the detector and the uniformity of pixel size and arrangement are also necessary. For astrometric observations, a Strehl ratio of 0.9, indicating an image close to the diffraction limit, is required. In transit observations, there is no stringent requirement for image sharpness, but uniformity of the detector is necessary. If saturation becomes an issue for bright objects due to sharp images during transit observations, adjustments can be made using the integration time or by utilizing the drift scan mode, where the telescope pointing direction is slightly moved during exposure.

The next requirement is a highly stable telescope optical system. The telescope inevitably has image distortion within its field of view (FOV) to some extent. Additionally, since the optical system in orbit will inevitably have slight deviations from its design values, the distortion will also be affected by these deviations. In the step-stare method, the telescope's pointing direction is moved within a range smaller than the FOV to capture images, and the relative positions of stars in the overlapping regions of different images are maintained over a short period. This allows for the estimation of distortion. For accurate distortion estimation, it is necessary that no changes in distortion occur during the estimation process, or if they do, only low-order changes with a limited number of parameters, such as a similarity transformation. Therefore, a highly stable telescope optical system is required. If there are temperature changes in the telescope's optical system, distortion is expected to change due to thermal contraction effects. Thus, it is necessary to minimize temperature fluctuations of the optical system in orbit. Similarly, variations in the sensitivity of the detector and in pixel size and arrangement must also be limited to low-order changes with a limited number of parameters. In transit observations, there are no stringent requirements regarding this aspect.

By observing the photospheric emissions of stars in the central region of our Galaxy, the positions of these stars can be accurately measured. For this positional measurement, observations in the visible to near-infrared range, where photospheric emissions are dominant, are suitable. Far-infrared, radio, or high-energy emissions are not suitable for positional measurements because they often include significant emissions from non-stellar sources. Within the visible to near-infrared range, observations in the infrared region are preferred due to the less severe interstellar extinction from the Earth to the Galactic center compared to the visible wavelength range, which suffers from significant attenuation. Therefore, the optimal observational wavelength range is around 1 – 2 $\mu\text{m}$ .

We are developing a two-dimensional detector using InGaAs with an enhanced radiation-resistant design for use in this wavelength range.<sup>3</sup> When cooled, the long-wavelength end of its sensitivity extends to approximately 1.6  $\mu\text{m}$ . To avoid significant differences in the PSF shape due to the color of the stars, caused by diffraction effects dependent on the observation wavelengths, the short-wavelength end is set to approximately 1.0  $\mu\text{m}$ . We define the observational wavelength range as the *Hw* band. The conversion formula from the *J* and *H* bands to the *Hw* band is as follows:

$$Hw = 0.9J + 0.1H - 0.06(J - H)^2$$

From the perspective of the available launch vehicle cost constraints, a near-Earth orbit is chosen. To achieve a highly stable telescope by obtaining a stable thermal environment, a SSO with LTAN at 6:00 or 18:00 is selected. Considering the limitations of the launch conditions and the need to ensure a sufficient Earth avoidance angle (the angle between the telescope’s pointing direction and the Earth’s limb) during observations of the Galactic center, a high altitude is preferable. Thus, the orbital altitude is set to approximately 600 km.

To maximize the continuous observation time of specific targets in a SSO with LTAN at 6:00 or 18:00, the operational attitude shown in Figure 1 is adopted. The sunshield is deployed towards the Sun, maintaining an angle within 45 degrees between the Sun and the sunshield. This configuration allows for the observation of the same object for approximately half an orbit. When the pointing direction is perpendicular to the geocentric direction, the Earth avoidance angle at an altitude of 600 km is 23.9 degrees. To avoid the effects of stray light from the Earth, the telescope is equipped with a baffle, and the evaluation of stray light assumes an Earth avoidance angle of 23 degrees or more.

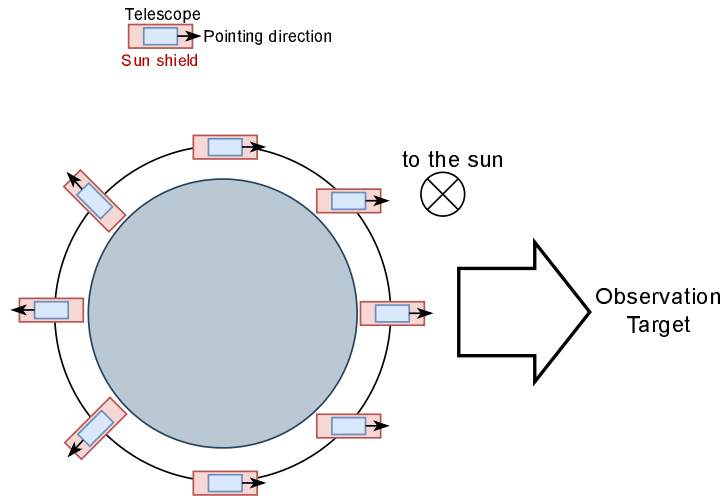


Figure 1. Specific observational attitude

As shown in Figure 2, observations of the Galactic center region will be conducted during two seasons: spring and autumn. In winter, the direction of the Sun coincides with the direction of the Galactic center, making observations impossible. In summer, sunlight shines from the opposite direction of the telescope’s pointing direction, and maintaining the satellite’s thermal environment under these conditions is expected to exceed cost constraints. Therefore, observations of the Galactic center region will not be conducted in summer.

For astrometric observations, it is necessary to resolve the motion parameters of the apparent helical motion of stars, which include annual parallax and proper motion. To facilitate the resolution of the degeneracy between the apparent elliptical motion with an annual period and linear proper motion, a minimum observation span of 1.5 years is required. Furthermore, to achieve the required precision for astrometric parameters, a scientific observation period of 3 years, with observations conducted for six months each year, is necessary for astrometric measurements. On the other hand, for the exploration of exoplanets, a minimum total observation period of at least 14 months is required. If the observation time allocation ratio between astrometric observations and exoplanet exploration is 1:1, a total observation period of 28 months is required to complete the exoplanet exploration. Considering these factors, the total scientific observation period is set to 3 years.

#### 4. BASIC PARAMETERS AND ERROR BUDGETING

The basic parameters of JASMINE are listed in Table 1. Here,  $\alpha$  represents the ratio of the pixel scale to Nyquist sampling, and it is expressed as follows using the focal length  $f$ , reference wavelength  $\lambda_{\text{ref}}$ , EPD  $D$ , and pixel size  $p$ :

$$\alpha = \left( \frac{p}{f} \right) / \left( \frac{\lambda_{\text{ref}}}{2D} \right)$$

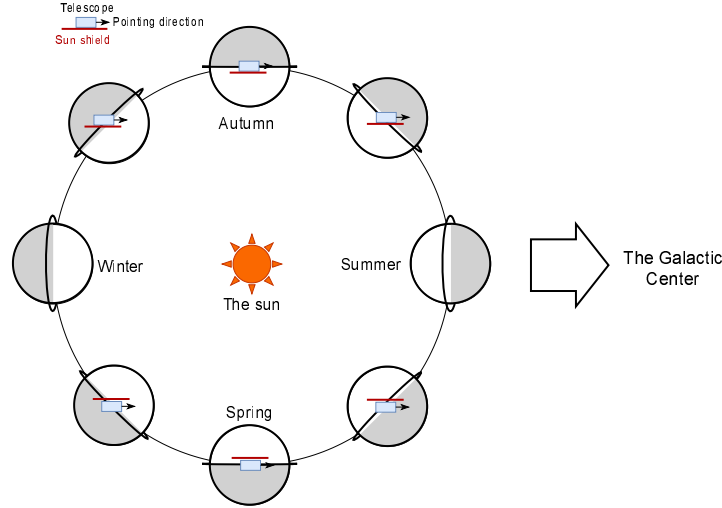


Figure 2. The period of Galactic center observations

Table 1. Basic parameters of JASMINE

Effective Pupil Diameter (EPD)	$D$	36 cm
Number of pixels per detector chip	$N_{\text{pix}}$	$1952 \times 1952$
Number of detector chips	$N_d$	4
Reference wavelength	$\lambda_{\text{ref}}$	$1.3 \mu\text{m}$
Ratio of pixel scale to Nyquist sampling	$\alpha$	1.27
Single shot exposure time	$t_{\text{exp}}$	12.5 sec

#### 4.1 Error Budgeting

Here, we demonstrate that JASMINE meets the required specifications by using the above parameters along with estimated values for various efficiencies. Furthermore, we discuss the allocation of errors.

To observe over 2,400 stars in the Galactic center in the  $H\alpha$  band, it is necessary to observe stars of magnitude 12.5 or brighter. For over 45,000 stars in the Galactic center, stars of magnitude 14.5 or brighter need to be observed. The positional accuracy is roughly proportional to the square root of the number of photons received from the stars, resulting in an approximate factor of 2.5 difference for a two-magnitude difference. Specifically, if the accuracy is  $40 \mu\text{as}$  at magnitude 12.5, it would be approximately  $100 \mu\text{as}$  at magnitude 14.5. Therefore, it is sufficient to determine the telescope parameters based on the achievable accuracy at magnitude 12.5. In this paper, parameters that can achieve the extra success criterion of  $25 \mu\text{as}$  will be considered.

First, we determine the theoretical value of the achievable stellar positional accuracy.

The positional accuracy per signal photon is given by the following equation:

$$\sigma_{\text{single}} = \frac{\lambda_{\text{ref}}}{D} [\text{rad}]$$

Observations of the Galactic center region are allocated to the observation season for half of the year and to observation time for half of the orbital period. Therefore, the observation time  $T_{\text{obs}}$  for a single celestial object, given the scientific observation operation period  $T_{\text{ope}}$ , is approximately as follows:

$$T_{\text{obs}} = \kappa \eta \frac{T_{\text{ope}}}{4}$$

Here,  $\kappa$  is the temporal observation efficiency, which accounts for unavoidable dead time and maneuver time required for detector operations, as well as the time required for calibration operations, subtracted from the total

observation time.  $\eta$  is the coverage rate of a single-shot exposure over the area to be observed ( $A_{\text{obs}}$ ) in the Galactic center region.

$$\eta = N_d N_{\text{pix}} \left( \frac{\alpha \lambda_{\text{ref}}}{2D} \right)^2 / A_{\text{obs}}$$

To estimate the number of observation shots per celestial object, assuming an imaging cycle time slightly longer than the exposure time, approximately 14 sec, we obtain approximately  $N_s = 7.7 \times 10^4$ .

Then, the total number of electrons obtained throughout the entire observation period for a single celestial object is given by:

$$\begin{aligned} N_{\text{total}} &= \beta \frac{\pi}{4} D^2 F_{12.5} \times \frac{\kappa \eta T_{\text{ope}}}{4} \\ &= \frac{\pi}{16} \beta D^2 F_{12.5} \kappa N_d N_{\text{pix}} \left( \frac{\alpha \lambda_{\text{ref}}}{2D} \right)^2 \frac{1}{A_{\text{obs}}} T_{\text{ope}} \\ &= \frac{\pi \beta \kappa \alpha^2 N_d N_{\text{pix}}}{64 A_{\text{obs}}} F_{12.5} \lambda_{\text{ref}}^2 T_{\text{ope}} \end{aligned}$$

here,  $F_{12.5}$  is the number of photons from a star of 12.5 magnitude in the  $Hw$  band and  $\beta$  is the product of the entrance pupil's obstruction ratio, optical system efficiency, and detector quantum efficiency.

Therefore, the positional accuracy is theoretically given by the following

$$\begin{aligned} \sigma_{\text{final}} &= \frac{\sigma_{\text{single}}}{\sqrt{N_{\text{total}}}} \\ &= 11.4 \left( \frac{36 \text{ [cm]}}{D} \right) \frac{1}{\sqrt{\left(\frac{\beta}{0.5}\right) \left(\frac{\kappa}{0.5}\right) \left(\frac{\alpha}{1.0}\right) \sqrt{\left(\frac{N_d}{4}\right) \left(\frac{N_{\text{pix}}}{1952 \times 1952}\right) \sqrt{\left(\frac{T_{\text{ope}}}{3 \text{ [year]}}\right)}}}} \text{ [\mu as]} \end{aligned}$$

Here, unlike in Table 1,  $\alpha$  is taken as 1 for Nyquist sampling, and both  $\beta$  and  $\kappa$  are assumed to be 0.5, allowing the position measurement error to be approximately 12  $\mu\text{as}$ . Using this value as a starting point, we consider the error budget. In the step-stare method, the distortion correction is performed using the acquired data itself. At this time, an amount of  $\sigma_d = 10 \mu\text{as}$ , comparable to  $\sigma_{\text{final}}$  is allocated as the correction error for distortion. Additionally, an unknown error  $\sigma_u$  of the same magnitude, 10  $\mu\text{as}$ , is assumed at this stage. These errors are considered to be independent and are combined using the root sum of squares. It is also assumed that the reduction in error due to multiple exposures is effective as the square root of the number of observations. Therefore, the requirement for the position determination error in a single shot,  $\sigma_{\text{ss}}$ , relative to the extra success requirement,  $\sigma_{\text{req}}$ , is given by the following

$$\begin{aligned} \sigma_{\text{req}}^2 &\geq \frac{\sigma_{\text{ss}}^2}{\sqrt{N_s}} + \sigma_d^2 + \sigma_u^2 \\ \sigma_{\text{ss}} &\simeq 5.7 \times 10^3 \text{ [\mu as]} \end{aligned}$$

Furthermore, by setting a margin that adds an error of the same magnitude to the single-shot error, this value is divided by the square root of 2 to determine the target error as follows.

$$\sigma_{\text{target}} \simeq 4 \text{ [mas]}$$

Table 2. The list of parameters, the final adopted values, and comments on the exploration range

parameter	adopted value	comment
EPD	350 mm	Test 350 to 400 mm. A smaller size reduces costs.
Cobs	0.35	Central obscuration ratio. This is set to the designed value.
Spider	tripod width 5 mm	Fixed
Wavelength range	1.0 – 1.6 $\mu\text{m}$	Fixed
Optical efficiency	0.88	Constant across all wavelengths
readout noise	15 electrons	Test 5 to 40 electrons
dark current	75 e <sup>-</sup> /sec/pix	Test 10 to 120 e <sup>-</sup> /sec/pix
Qe	0.75	Detector quantum efficiency, test 0.5 to 0.8
flat	0.01	Pixel to pixel sensitivity difference, test 0 to 0.03
$\sigma_{\text{ACE}}$	0.3 arcsec	Attitude control error within a single shot, test 0.15 to 0.45 arcsec
$t_{\text{exp}}$	12.5 sec	Single shot exposure time
Rv	3.1	Ratio of total to selective extinction
$J-H$	2	$J-H$ color of the target star
Strehl ratio	0.90	Test 0.85, 0.90, 0.95, 1.0

## 4.2 Parameter search

Using the scalar wave theory for optical calculations and the least squares method for error estimation, we derived the relationship between various parameters (Table 2) and the position determination error obtained in a single shot.

First, the intensity of the scalar wave at the entrance pupil plane was given by setting the transmittance of the unobstructed regions to 1, and the regions obstructed by the spider and central obstruction to 0. Furthermore, phase differences were introduced to the incident wave using sample values of wavefront errors (WFE) in the optical system deviating from the ideal design values. By performing a Fourier transform of this scalar wave at the entrance pupil plane, we calculated the optical point spread function (PSF) at the focal plane. The disturbance in the telescope's pointing direction was then added as a Gaussian convolution to obtain the PSF at the focal plane. This PSF was calculated at a finer scale than the pixel scale to determine the number of generated electrons at each pixel. Additionally, derivatives with respect to the focal plane coordinates were computed using differences, given the finer scale PSF.

The optical PSF was calculated for each wavelength, adjusted to match the scale at the focal plane, and combined according to the wavelength intensity distribution of the celestial object.

The center position of the point source  $(\mu_x, \mu_y)$  on the detector and the observed image coordinates  $(x, y)$  are represented as  $P(x, y; \mu_x, \mu_y)$  on the detector. By indexing the detector pixels, the model of the observed values is expressed as follows, considering the coefficient  $\varepsilon$  corresponding to the brightness of the point source and the background signal  $B$ :

$$F_i = \varepsilon \int_i P(x, y; \mu_x, \mu_y) dx dy + B$$

Here, the integral represents the integration within the  $i$ -th pixel. Both the coefficient  $\varepsilon$  and the background  $B$  are assumed to be constant across pixels. Rewriting the integral notation, we express it as follows:

$$F_i = \varepsilon P_i(\mu_x, \mu_y) + B$$

Considering a small displacement of the center position of the point source,

$$\mu_x = \mu_{x0} + \delta\mu_x$$

$$\mu_y = \mu_{y0} + \delta\mu_y$$

and linearizing, we obtain:

$$F_i = P_i(\mu_{x0}, \mu_{y0})\varepsilon + \beta + \varepsilon \partial_{\mu_x} P_i(\mu_{x0}, \mu_{y0}) \delta\mu_x + \varepsilon \partial_{\mu_y} P_i(\mu_{x0}, \mu_{y0}) \delta\mu_y$$

Thus, the linearized model equation is obtained.

The error matrix, assuming no correlation and no bias among the pixels, consists only of diagonal components. The error for the  $i$ -th pixel is given by the contributions from shot noise, readout noise ( $\sigma_{\text{readout}}$ ), and flat noise ( $\sigma_{\text{flat}}$ ), as follows:

$$\sigma_i^2 = \varepsilon P_i(\mu_x, \mu_y) + B + \sigma_{\text{readout}}^2 + \sigma_{\text{flat}}^2$$

The contribution of flat noise is given by:

$$\sigma_{\text{flat}} = \gamma \varepsilon P_i(\mu_x, \mu_y)$$

where  $\gamma$  is the pixel to pixel sensitivity difference value given as the flat error.

From the above observation model equation, the estimated error matrix of the parameters is obtained as an elliptical error circle in the focal plane coordinates using the least squares estimation method. The estimation error is determined by using the value in the major axis direction of the position determination error from this error matrix. In the report by Kamizuka et al.,<sup>4</sup> the modeling conducted here is further advanced, and error estimation is performed using the Monte Carlo method.

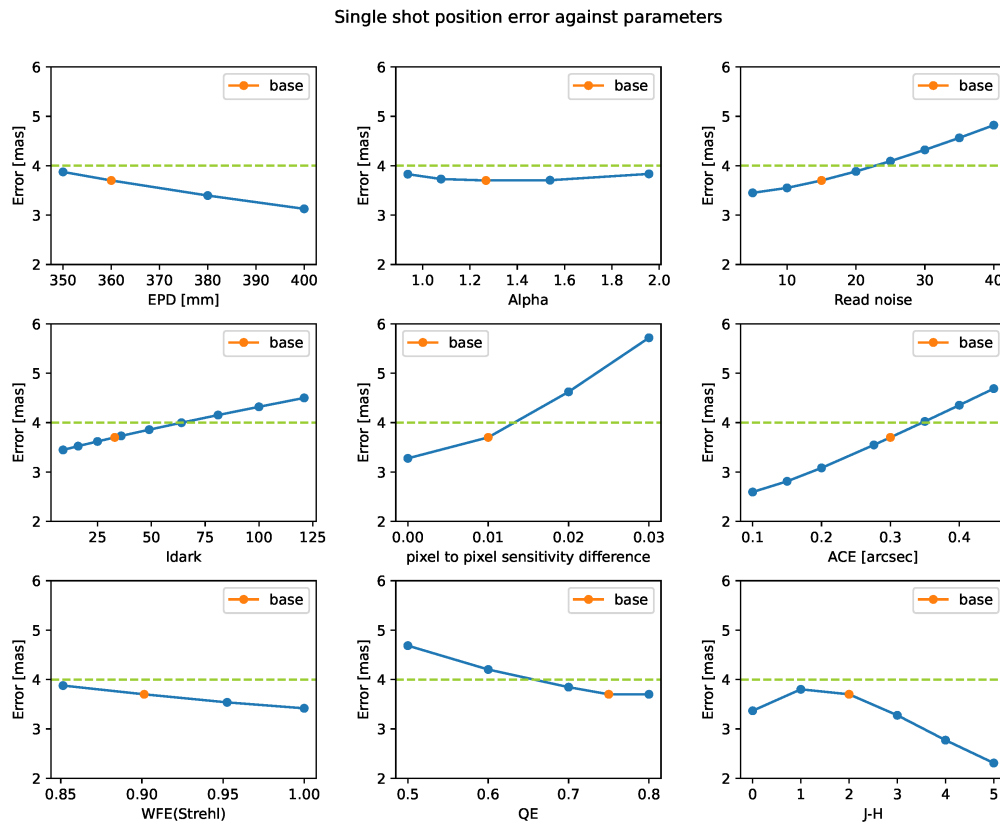


Figure 3. Dependency of the position estimation error on various parameters. "base" refers to the values corresponding to the adopted parameters. The adopted values can be found in Table 2.

Figure 3 illustrates the dependency of the position determination error on various parameters in a single shot. Although the lower limit for the aperture diameter is 350 mm, it is set to 360 mm to allow for some margin. The focal length is determined by the value of alpha, but it does not have a significant impact on a



single shot. The adopted values for readout noise, dark current, pointing direction disturbances (ACE), pixel sensitivity uniformity, Strehl ratio, and detector quantum efficiency are sufficient. The color of the stars, with an expected  $J - H$  value of 2 magnitudes or more for stars in the Galactic center region, shows that the redder the stars, the smaller the error.

## 5. SUMMARY

This paper outlines how the basic concept of JASMINE was derived from scientific requirements. It presents the estimation of errors and the approach to error allocation necessary to meet these requirements, as well as the parameters and estimated errors of the observational equipment. The adopted values are set to achieve the extra success level. The JASMINE project is being advanced based on this basic concept. For an examination of whether image distortion falls within the allocated error budget, refer to Isobe et al.<sup>5</sup> For details on the assembly and testing of the telescope, refer to Suematsu et al.<sup>6</sup> Further information on the analysis of data obtained through the step-stare method can be found in Ohsawa et al.<sup>7</sup>

## REFERENCES

- [1] Gaia Collaboration, “The Gaia mission,” *Astronomy & Astrophysics* **595**, A1 (Nov. 2016).
- [2] Kawata, D., Kawahara, H., Gouda, N., Secrest, N. J., Kano, R., Kataza, H., Isobe, N., Ohsawa, R., Usui, F., Yamada, Y., Graham, A. W., Pettitt, A. R., Asada, H., Bekki, K., Dorland, B. N., Fujii, M., Fukui, A., Hattori, K., Hirano, T., Kamizuka, T., Kashima, S., Kawanaka, N., Kawashima, Y., Klioner, S. A., Kodama, T., Koshimoto, N., Kotani, T., Kuzuhara, M., Levine, S. E., Majewski, S. R., Masuda, K., Matsunaga, N., Miyakawa, K., Miyoshi, M., Morihana, K., Nishi, R., Notsu, Y., Omiya, M., Sanders, J., Tanikawa, A., Tsujimoto, M., Yano, T., Aizawa, M., Arimatsu, K., Biermann, M., Boehm, C., Chiba, M., Debattista, V. P., Gerhard, O., Hirabayashi, M., Hobbs, D., Ikenoue, B., Izumiura, H., Jordi, C., Kohara, N., Löffler, W., Luri, X., Mase, I., Miglio, A., Mitsuda, K., Newswander, T., Nishiyama, S., Obuchi, Y., Ootsubo, T., Ouchi, M., Ozaki, M., Perryman, M., Prusti, T., Ramos, P., Read, J. I., Rich, R. M., Schönrich, R., Shimizu, R., Shikauchi, M., Suematsu, Y., Tada, S., Takahashi, A., Tatekawa, T., Tatsumi, D., Tsujimoto, T., Tsuzuki, T., Urakawa, S., Uraguchi, F., Utsunomiya, S., van Eylen, V., van Leeuwen, F., Wada, T., and Walton, N. A., “JASMINE: Near-Infrared Astrometry and Time Series Photometry Science,” *PASJ: Publications of the Astronomical Society of Japan*, 020 (Apr 2024).
- [3] Miyakawa, K., Tada, S., Kataza, H., Kano, R., Wada, T., Ozaki, M., Kotani, T., Kawahara, H., Usui, F., and Kasagi, Y., “Performance report of a substrate-removed ingaas sensor for the JASMINE mission,” *Society of Photo-Optical Instrumentation Engineers (SPIE) Conference Series* (2024).
- [4] Kamizuka, T., Kawahara, H., Ohsawa, R., Kataza, H., Kawata, D., Yamada, Y., Hirano, T., Miyakawa, K., Aizawa, M., Omiya, M., Yano, T., Kano, R., Wada, T., Löffler, W., Biermann, M., Ramos, P., Isobe, N., Usui, F., Hattori, K., Yoshioka, S., Tatekawa, T., Izumiura, H., Fukui, A., Miyoshi, M., Tatsumi, D., and Gouda, N., “JASMINE image simulator for high-precision astrometry and photometry,” *Society of Photo-Optical Instrumentation Engineers (SPIE) Conference Series* (2024).
- [5] Isobe, N., Kashima, S., Suematsu, Y., Gouda, N., Kano, R., Kataza, H., Kawahara, H., Kohara, N., Kondo, I., Mase, I., Ohsawa, R., Tsuzuki, T., Usui, F., Utsunomiya, S., Wada, T., Yamada, Y., Yano, T., Takahashi, A., Hattori, T., Takeda, K., and Arima, Y., “Structural, thermal, and optical stability of the JASMINE telescope system,” *Society of Photo-Optical Instrumentation Engineers (SPIE) Conference Series* (2024).
- [6] Suematsu, Y., Tsuzuki, T., Kohara, N., Isobe, N., Kataza, H., Kashima, S., and Kano, R., “Evaluation and verification plan for JASMINE telescope optics on the ground,” *Society of Photo-Optical Instrumentation Engineers (SPIE) Conference Series* (2024).
- [7] Ohsawa, R., Kawata, D., Kamizuka, T., Yamada, Y., Löffler, W., and Biermann, M., “Concept verification of the JASMINE astrometric plate analysis,” *Society of Photo-Optical Instrumentation Engineers (SPIE) Conference Series* (2024).